

Original Article

Qualitative study for finasteride detection in the prostate delivered by reversible inhibition of sperm under guidance – Prostate hair (RISUG-PH™) was injectable implant

Santosh Gupta¹, Jovana Bisevac², Sujoy K. Guha³

¹School of Medical Science and Technology, Indian Institute of Technology, Kharagpur, West Bengal, India, ²Center for Eye Research and Innovative Diagnostics, Department of Ophthalmology, Institute for Clinical Medicine, Faculty of Medicine, University of Oslo, Oslo, Norway, ³Centre for Biomedical Engineering, Indian Institute of Technology Delhi, New Delhi, India.



*Corresponding author:

Sujoy K. Guha,
Centre for Biomedical
Engineering, Indian Institute of
Technology Delhi, New Delhi,
India.

guha_sk@yahoo.com

Received: 12 February 2024

Accepted: 07 February 2025

Published: 18 April 2025

DOI

[10.25259/JRHM_2_2024](https://doi.org/10.25259/JRHM_2_2024)

Quick Response Code:



Supplementary link:

https://doi.org/10.25259/JRHM_2_2024

ABSTRACT

Objectives: Drug delivery to the prostate through the conventional route is associated with pharmacokinetics-based and drug-related side effects. Finasteride (FIN) is the model drug used clinically for the management of prostate hyperplasia through the oral route. An alternate localized drug delivery route is a prerequisite that may offer many advantages over the oral route of drug delivery to the prostate. The present study confirms the hypothesis of using vas deferens, a localized drug delivery route to the prostate using an injectable drug delivery implant, that is, Reversible Inhibition of Sperm Under Guidance – Prostate Hair (RISUG-PH™).

Material and Methods: We developed a styrene maleic anhydride, FIN, and dimethyl sulfoxide-based injectable implant that was biophysically characterized using Fourier transform infrared (FTIR) and powder X-ray diffraction (PXRD). Fluorescence microscopy and atomic force microscopy (AFM) were used to characterize the implant. Matrix-assisted laser desorption ionization–time of flight (MALDI-ToF/ToF) and high-resolution mass spectrometry (HRMS) were used to confirm the presence of FIN in the prostate of the implant-injected rats.

Results: FTIR and powder-XRD confirmed the amorphous nature of the implant. Fluorescence microscopy and AFM confirmed the *in vivo* generation of sub-micron-sized particles, which may act as a drug carrier forming from the implant. Finally, using MALDI-ToF/ToF and HRMS, the presence of FIN was confirmed in the ventral prostate of male rats by identifying the m/z ratio corresponding to the production of molecular FIN and confirming the elemental composition of the detected [M+H]⁺ precursor ion with standard FIN within an acceptable limit of actual mass error of –7.2 ppm versus +3.5 ppm of standard FIN, respectively. FIN was also detected in the prostate after a period of 28 days post 1-time implant injection in the lumen of vas deferens of the male rats. It showed a better signal intensity detection of FIN compared to the oral route.

Conclusion: This study confirmed that RISUG-PH™ delivers FIN to the prostate on single implantation in male rats, confirming the use of vas deferens as a localized route for drug delivery to the prostate.

Keywords: Drug delivery system, Finasteride, Prostate, RISUG PH™, Vas deferens

INTRODUCTION

Prostate-related disease is one of the most pertinent problems in urology, affecting millions of males across the globe. Prostate cancer and benign prostate hyperplasia has higher burden rate in aging males, causing a series of problems that affect the life standards of the patients.^[1,2]

This is an open-access article distributed under the terms of the Creative Commons Attribution-Non Commercial-Share Alike 4.0 License, which allows others to remix, transform, and build upon the work non-commercially, as long as the author is credited and the new creations are licensed under the identical terms.

©2025 Published by Scientific Scholar on behalf of Journal of Reproductive Healthcare and Medicine

The conventional approach to managing these prostate-related diseases primarily involves pharmacological interventions that are delivered through systemic circulation, typically through oral routes or systemic injections. While these methods have been the gold standard for treatment, they are not without drawbacks.^[3] Systemic administration of drugs often results in a variety of side effects, particularly in the case of chemotherapy for prostate cancer.^[3] Adverse effects may include but are not limited to, erectile dysfunction, depression,^[4,5] and cardiovascular complications, particularly with long-term use of medications for BPH management. These challenges underscore the pressing need for alternative drug delivery routes to mitigate systemic administration's adverse effects while maintaining therapeutic efficacy.^[6-8]

One promising avenue for localized drug delivery involves the vas deferens, a structure traditionally recognized for its role in sperm transport and fluid secretion. Beyond its reproductive functions, the vas deferens have been implicated in the transport of small molecules and larger particles, influencing the physiology of the male reproductive tract and the maintenance of secondary sex organs such as the prostate and seminal vesicles.^[9,10] Earliest studies, such as those conducted by Skinner and Rowson^[11] have proposed that the luminal transport mechanisms within the vas deferens could play a crucial role in maintaining the health and functionality of the male reproductive system, particularly through the delivery of testicular fluid containing testosterone to the ampulla. This concept was further supported by research from Ohtani and Gannon in 1982,^[12] which examined the microvasculature of the rat vas deferens and suggested a potential pathway for luminal transport mechanisms to influence prostate maintenance.

Pierpoint and Davies^[13] showed the role of the vas deferens in maintaining prostate health, indicating that while venous drainage may play a significant role, the luminal transport mechanisms are equally important. Collectively, these foundational studies highlight the vas deferens as a critical conduit that may facilitate localized drug delivery to the prostate, thereby hyperplasia offering a novel approach to the treatment of prostate-related diseases.^[13-15]

In this context, the development of Reversible Inhibition of Sperm Under Guidance (RISUG®) presents a groundbreaking advancement in male contraceptive technology.^[16,17] RISUG is a polymer-based formulation that, on injection into the lumen of the vas deferens, interacts with the vas fluid to form a biocompatible hydrogel. This gel, composed of a copolymer of styrene maleic anhydride (SMA) dissolved in dimethyl sulfoxide (DMSO), acquires a polyelectric nature that disrupts sperm cell membranes, effectively rendering them non-viable. The contraceptive efficacy of RISUG has been attributed to its ability to rupture the plasma membranes of sperm cells and release enzymes critical for fertilization.

Building on the principles of RISUG, the Reversible Inhibition of Sperm Under Guidance – Prostate Hair (RISUG-PH™) implant^[18] has been engineered for targeted drug delivery to the prostate. This innovative system utilizes a combination of high-molecular-weight and low-molecular-weight SMA, where the former provides stability at the injection site, and the latter facilitates the gradual release of drug components over time. The incorporation of phospholipids derived from dead sperm cell membranes further enhances the functionality of this delivery system, leading to the formation of a multicomponent system within the vas deferens. Our hypothesis posits that this system can encapsulate nano-sized polymer-drug complexes, culminating in the formation of what we term “Invivgensome,” a novel drug delivery system (DDS) designed to achieve localized pharmacological action within the prostate.

The present study aims to explore the feasibility of localized drug delivery to the prostate through the vas deferens using a uniquely formulated DDS comprised SMA-Finasteride (FIN)-DMSO. We seek to determine whether pharmacologically active molecules can effectively reach the prostate over an extended period, thereby offering a potential therapeutic advantage over traditional systemic administration methods. Furthermore, this research provides the first experimental evidence supporting the notion that nanoparticles can form within the body, specifically within the vas deferens, mediated by our innovative DDS.

MATERIAL AND METHODS

Materials

FIN (F1293) was purchased from Sigma-Aldrich, SMA was obtained from the RISUG Pilot Plant (Indian Institute of Technology, Kharagpur, India), Nile Red (72485) from Sigma-Aldrich, Germany, high-performance liquid chromatography (HPLC) grade acetonitrile, methanol, and ammonium acetate were purchased from Merck, Germany. HPLC grade methyl tertiary butyl ether (MTBE) and DMSO were purchased from Spectrosol, India. 4-(2-Hydroxyethyl) piperazine-1-ethanesulfonic acid sodium salt, N-(2-Hydroxyethyl) piperazine-N'-(2-ethanesulfonic acid) sodium salt HEPES (H8651) was purchased from Sigma. Formic Acid, 2,5-Dihydroxybenzoic acid (DHB) Trifluoroacetic acid (TFA) from Sigma Aldrich, USA. All chemicals were used as obtained without further purification. Milli-Q water obtained from Milli-Q Integral 3 system (Millipore, France) was used for all experiments.

Animal maintenance and condition

With the approval of the Institutional Animal Ethics Committee, mature male albino rats (Wistar strain) of weight between 150 g and 200 g were used in these studies. The minimum age for male rats to become sexually active

is 90 days;^[19] hence, the rats used in the studies were between 5 and 6 months old. Albino rats were kept at the animal house of the School of Medical Science and Technology, IIT, Kharagpur, India, under conditions as per recommendations of the Institutional Animal Ethics Committee. Animals were maintained at approximately 25°C and 65% humidity with a 12-h light–12-h dark cycle and were fed with standard food and water *ad libitum*.

Methods

Synthesis of SMA: FIN: DMSO DDS/implant

The DDS used in this study was synthesized according to the methods described in United States patent number WO/2013/124865.^[16] SMA polymer, having weight average molecular weight between 250kD and 400kD, was used for the formulation of the DDS. The molecular weight was determined by gel permeation chromatography at 35°C (Viscotek, Malvern, USA). Briefly, the three components of the DDS were taken in weight ratio of 1:0.5:10 and 1:1:10 for SMA, FIN, and DMSO, respectively. The synthesis process involved two steps. In the first step, 30% of DMSO was taken and the weight amount of FIN was added and mixed properly. To the dissolved mixture, a weight amount of SMA was added and allowed to mix and simultaneously heated at 75°C to about 4 h in a nitrogen environment with intermittent stirring. In the second step, after completion of the heating, the resulting 70% of the DMSO was added and mixed. The final mixture was stirred intermittently and heated at 75°C for 2 h [Figure 1]. The final prepared mixture formed a viscous liquid, which was used in this paper as a DDS/implant.

Animal surgery

The injection of the implant was followed based on our earlier method.^[20] Briefly, the rats were anesthetized, hairs were removed from the scrotal region, and sterilized with betadine (Povidone Iodine), followed by cleaning with sterile

water. A vertical medial incision was made in the scrotal sac, and the vas deferens were pulled out after locating it. 20 μ L of the implant was injected toward the distal direction (prostate end) of the vas deferens. One drop of sterile water for injection was dropped at the injection site to precipitate the polymer and close the injection site. The polymer-drug implant was injected bilaterally following the same protocol. After the injection, the scrotal sac incision was stitched, and the wound was dressed to maintain an aseptic condition.

Characterization of DDS by Fourier transform infrared (FTIR) and powder X-ray diffraction (PXRD)

FTIR spectroscopy

FTIR analysis of the FIN, SMA, DMSO, and the implant was performed in a Perkin Elmer Instrument Spectrum Rx. Spectra were recorded in transmittance mode by the KBr pellet method with 256 scans and 1 cm^{-1} resolution.

PXRD

PXRD patterns were recorded with a Bruker AXS D8 ADVANCE diffractometer with a Cu Ka radiation source. The diffractograms were recorded in the 2θ angle range between 10° and 70°.

Sample preparation – the mixture consisting of FIN: DMSO, SMA: DMSO, and SMA: FIN: DMSO (1:1:10 and 1:0.5:10) ratio, which were loaded onto 1 \times 1 cm^2 glass slide and dried in a vacuum desiccator for 24 h at 30°C to obtain dried films which were used for PXRD analysis.

Characterization of the *in vivo* formed lipid particles

Fluorescence microscopy

To realize the concept of *in vivo* formed nanoparticles from the DDS, fluorescence imaging was executed under an inverted fluorescence microscope (Zeiss Observer Z1, Carl Zeiss, Oberkochen, Germany) at $\times 40$ oil objective configuration.

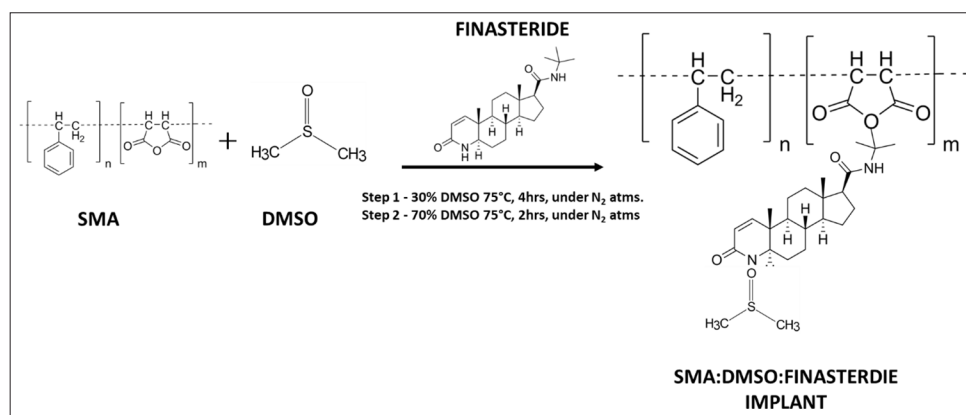


Figure 1: Schematic representation of the synthesis and development of SMA: DMSO: FIN drug delivery implant. SMA: Styrene maleic anhydride, DMSO: Dimethyl sulfoxide, FIN: Finasteride.

Nile Red fluorescent dye was used to study the *in vivo* formed nanoparticles.

Sample preparation – After sacrificing the rat, the vas deferens were excised, making an incision first at the distal end (toward the prostate) and then at the proximal end (toward the epididymis). The vas fluid from the lumen of both the vas per rat was squeezed out and diluted with 0.1M HEPES buffer (pH 7.2). The final suspension was short-spun in a benchtop Eppendorf microcentrifuge for 60 s at 12,000 relative centrifugal force (RCF) to sediment larger particles. From the supernatant, 25 μ L fluid was taken and spread on an 18 \times 18 mm glass substrate, followed by staining with Nile red dye (1:1000 in acetone) for 10 min. It was then washed with distilled water and mounted with distyrene, plasticizer, and xylene (DPX).

Atomic force microscopy (AFM)

Topography of the *in vivo* formed liposomes was investigated using AFM; Model 5100, Agilent Technologies, USA, in the intermittent contact mode with silicon cantilevers (PPPNCCL, Nanosensors, Inc., USA) having a force constant of 40 N/m and at a resonating frequency of 169.52 kHz. The height and diameter profile of the *in vivo* formed liposomes were assimilated by analyzing the AFM images using Pico Image Basic Software from Agilent Technologies.

Sample preparation – The vas fluid recovered after centrifugation was air-dried on a glass substrate and analyzed within 4 h of preparation.

Drug detection in ventral prostate by matrix-assisted laser desorption ionization-time of flight (MALDI-ToF/ToF) and high-resolution mass spectrometry (HRMS)

MALDI-ToF/ToF

MALDI ToF/ToF mass spectra were acquired using a Bruker ultrafleXtreme instrument equipped with smart beam-II™ laser technology (version 2-0-11-0) Nd/YAG (355 nm) with 2000-Hz tripled-frequency (Bruker Daltonics, Bremen, Germany). The excitation voltage was 20 kV, the reflector voltage was 20.83 kV, and the lens voltage was 7.17 kV. Laser strength was kept about 30% above the threshold for a good signal-to-noise ratio. All MS spectra were obtained in reflector-positive ion mode and processed using AutoFlex software provided by Bruker Daltonics (Bremen, Germany). At least 10 spots were averaged to get the final spectrum intensity for MS analysis. A variable number of shots was used to achieve the mass spectrometry/mass spectrometry (MS/MM) spectrum.

Sample preparation – FIN was extracted from the prostate tissue, adapting a liquid-liquid extraction process for the plasma sample as described by Constanzer *et al.* [21] with

some modifications. Briefly, the ventral prostate was excised, and fat was removed from it and washed with chilled saline water. The ventral prostate was pulverized with liquid nitrogen and homogenized using mortar and pestle in 4 mL of Milli-Q water and sonicated for 2 min (15 s pulse; 5 s relaxation; for eight cycles) at 50% amplitude. To the sonicated sample, 10 mL of MTBE was added and vortex mixed for 5 min. Then, the vial containing the sample was kept on an orbital shaker for 45 min. After incubation, the sample solution was centrifuged at 3500 g for 15 min at 4°C. Centrifugation caused the solution to separate into two phases. The upper organic phase was collected using a pipette. The resultant upper phase was dried under N₂ flow on a beaker containing water maintained at 50°C on a heating mantle. The dried extract was finally re-suspended in 300 μ L of acetonitrile. 2 μ L of the extract was mixed with 2 μ L of DHB (10 mg/mL in acetonitrile: water (50:50) in 0.1% TFA) and mixed thoroughly. The final mix was spotted on the MALDI plate and subjected to analysis.

HRMS

The elemental composition of FIN was analyzed using Xevo G2 TS HRMS from Waters. The system was equipped with a high-performance Zspray dual-orthogonal atmospheric pressure ionization (API) source with a quadrupole analyzer (MS1). Sample ionization was achieved in electro spray ionization (ESI) mode, and the data were acquired in positive ionization mode. The acquisition mode was MS scanning, and the spectra and the elemental composition were obtained from the MassLynx 4.1 software inbuilt with the system. The element limit used for studying FIN elemental composition was C: 0-30; H: 0-45; N: 0-5; O: 0-5 to detect the elemental composition of FIN ($C_{23}H_{36}O_2N_2 = M$; $C_{23}H_{37}O_2N_2 = M+H$). Actual mass error tolerance was set at 20.0 ppm.

Sample preparation – Drug extraction from the ventral prostate was similar to the liquid-liquid extraction method used for MALDI-ToF. After drying the organic phase, the final dried extract was resuspended in 2 mL of 50:50 ratio of acetonitrile: ammonium acetate in 0.1% formic acid. The final reconstituted sample was subjected to HRMS analysis without any further purification.

RESULTS

Characterization of DDS/Implant

Figure 2A shows the transmittance spectra of the entire component and the implant. Detailed IR transmittance and corresponding description of the molecular vibration and stretching are presented in Table 1. Pure FIN showed characteristic IR transmittance peak at 1687 cm^{-1} for the amide C=O stretching and 3429 and 3241 cm^{-1} for amide asymmetric and symmetric NH stretching vibration, respectively, 1600 was

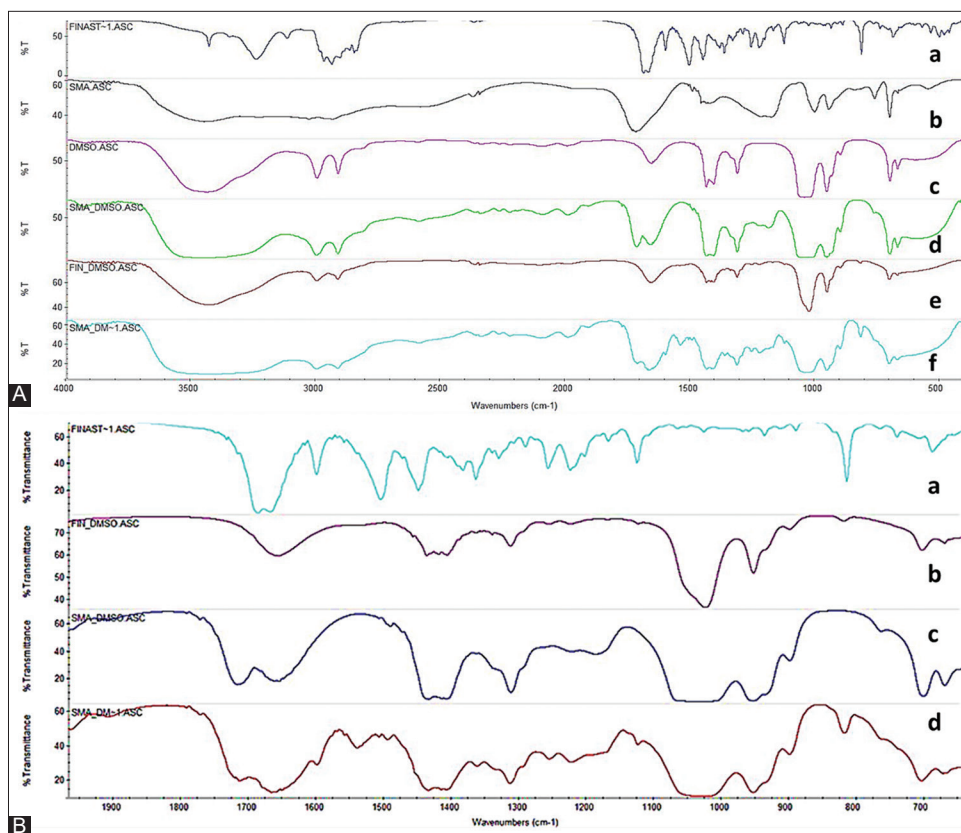


Figure 2: (A) FTIR Transmittance spectra of (a) FIN; (b) SMA; (c) DMSO; (d) SMA: DMSO; (e) FIN: DMSO; and (f) SMA: FIN:DMSO implant. FTIR: Fourier transform infrared, FIN: Finasteride, SMA: Styrene maleic anhydride, DMSO: Dimethyl sulfoxide. (B) FTIR spectrum of the fingerprint region of (a) FIN, (b) FIN: DMSO, (c) SMA: DMSO, and (d) SMA: FIN: DMSO. FTIR: Fourier transform infrared, FIN: Finasteride, SMA: Styrene maleic anhydride, DMSO: Dimethyl sulfoxide.

for C=C stretching vibration of the aromatic ring of FIN.^[22] The IR spectrum of DMSO exhibited peaks at 1437, 1407, and 1312 and a broad at around 1042 cm^{-1} . The peak at 1437 and 1407 corresponds to the antisymmetric bending of CH₃ ($\delta_{\text{as}}\text{CH}_3$), and the peak at 1312 is due to the symmetric deformation of the CH₃ group that is attached to the S atom. The broad peak around 1042 cm^{-1} can be assigned as S=O (ν_{SO});^[23,24] Moreover, IR spectra indicated the existence of water molecules in DMSO, which gave rise to a broad transmittance band around 3500 cm^{-1} due to O-H bond stretching vibration.

FTIR spectra of the SMA showed the characteristic transmittance at 1771 cm^{-1} for symmetric C=O anhydride stretching vibration, which was very weak. 1491.70 and 1450.47 bands are characteristic of styrene moieties. 1718 cm^{-1} was observed as characteristic of carboxylic acid.^[25] SMA-DMSO mixture showed characteristic transmittance bands at 954.51, 1036, 1312, 1663, and 2913.^[26,27] FIN and DMSO mixture transmittance spectra showed characteristic peaks 1025 cm^{-1} and 3422 cm^{-1} . The implant, which is a mixture of SMA, FIN, and DMSO in a particular ratio, showed a characteristic transmittance peak that was different

from either of the two physical mixtures of FIN+DMSO and SMA+DMSO [Figure 2B]. It showed characteristic peaks at 1667 cm^{-1} , 1223 cm^{-1} , 1600 cm^{-1} , and 1023 cm^{-1} .

PXRD is often used for evaluating polymer-drug interaction and the state of the drug in the polymer matrix. XRD pattern of SMA:DMSO [Figure 3a], FIN:DMSO [Figure 3b], SMA:FIN:DMSO (1:1:10) [Figure 3c] and SMA:FIN:DMSO (1:0.5:10) [Figure 3d]. The absence of any sharp peak in the polymer confirms the amorphous nature of the polymer. The XRD pattern of FIN dissolved in DMSO revealed high-intensity sharp diffraction peaks at 10.22, 14.20, 19.60, and 29.43 at 2θ [Figure 3b] which were indicative of its crystalline state. Pattern exhibited by the SMA:FIN:DMSO implant [Figure 3c] showed some peak characteristics of FIN but with a substantial decrease in intensity compared to the FIN diffractogram, suggesting the interaction of the FIN molecules with the SMA component of the implant. Interestingly, it was observed that the peak at $2\theta = 14.20$ and 29.43 disappeared with the decrease in FIN concentration with respect to SMA in the implant along with the decrease in intensity of the major peak at $2\theta = 19.60$ [Figure 3d].

Characterization of *in vivo* formed nano and submicron-sized particles

To understand the concept of *in vivo* generation of polymer-drug encapsulated lipid particles mediated by the implant injected in the lumen of vas deferens [Figure 4a], a fluorescence microscopic study was performed. Figure 4 represents the microscopic observation of the processed vas fluid squeezed from the excised vas of both control and

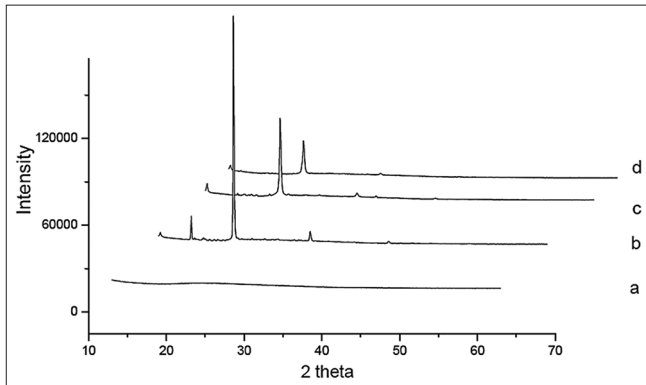


Figure 3: Powder X-ray diffraction of (a) SMA: DMSO; (b) FIN: DMSO; (c) SMA: FIN: DMSO (1:1:10); and (d) SMA: FIN: DMSO (1:0.5:10). FIN: Finasteride, SMA: Styrene maleic anhydride, DMSO: Dimethyl sulfoxide.

implant-injected rats. In [Figure 4b], the vas fluid did not show any particles in the sub-micron range, whereas, in the implant-injected rats, the vas fluid showed the presence of particles having sizes in the submicron range [Figure 4c].

The vas fluid extracted from the control rats did not show any such distinctive structures [Figure 5a (i) and (ii)]. The implant injected group showed the presence of nano and submicron-sized particles [Figure 5b (i) and (ii)]. The wavy patterned structures displayed in control groups were due to the film generated after the drying of the clear vas fluid on the glass substrate used for AFM sample preparation. In the implant-injected group, the globular particles had a diameter profile ranging from 100 nm to 700 nm. Figure 5c (i) and (ii) illustrate the dimension profile of two selected liposomal structures, which has a sub-micron size range.

FIN delivery and detection in ventral prostate

Gross ventral prostate weight in the implant injected group was 283.0 ± 4.726 mg in 14 days group and 210.3 ± 5.783 mg in 28 days group compared and were significantly different ($P > 0.005$) to the sham control 435.3 ± 7.311 mg [Figure S1 and Table S1]. MALDI-ToF MS and MS/MS analysis of standard solutions of FIN were carried out to obtain reference spectra for comparison with those obtained from prostate tissue extract of the implant-injected rats.

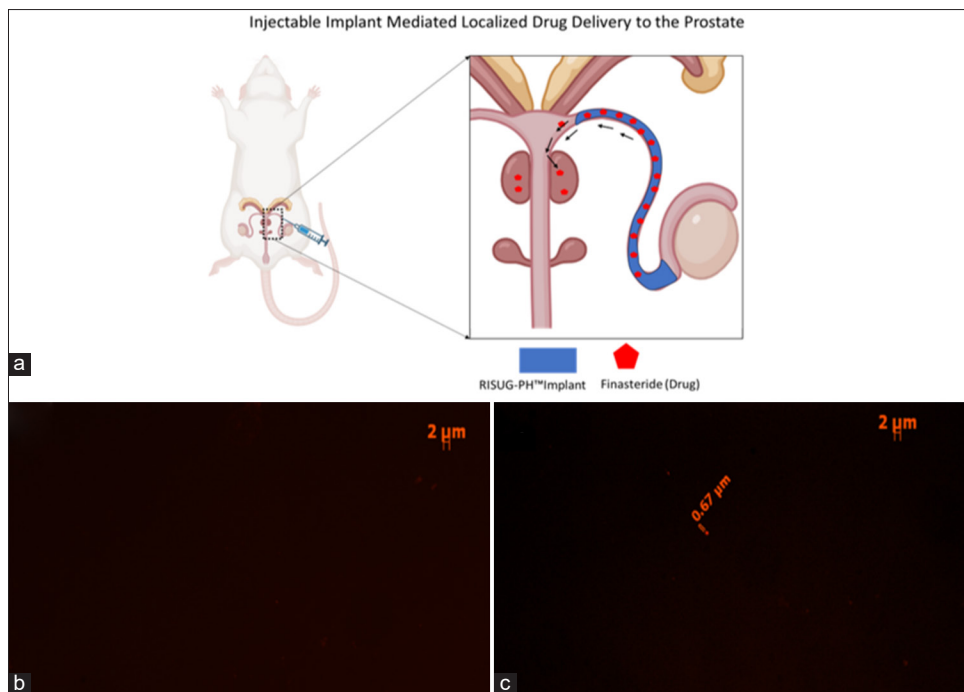


Figure 4: Fluorescence microscopy for detecting liposomal particles using Nile red staining of vas fluid extract of (a) control rat, (b) implant injected rat, (c) schematic representation of the proposed concept of implant mediated drug delivery to the prostate. Nanoparticles formed due to implant-sperm interaction carrying the drug.

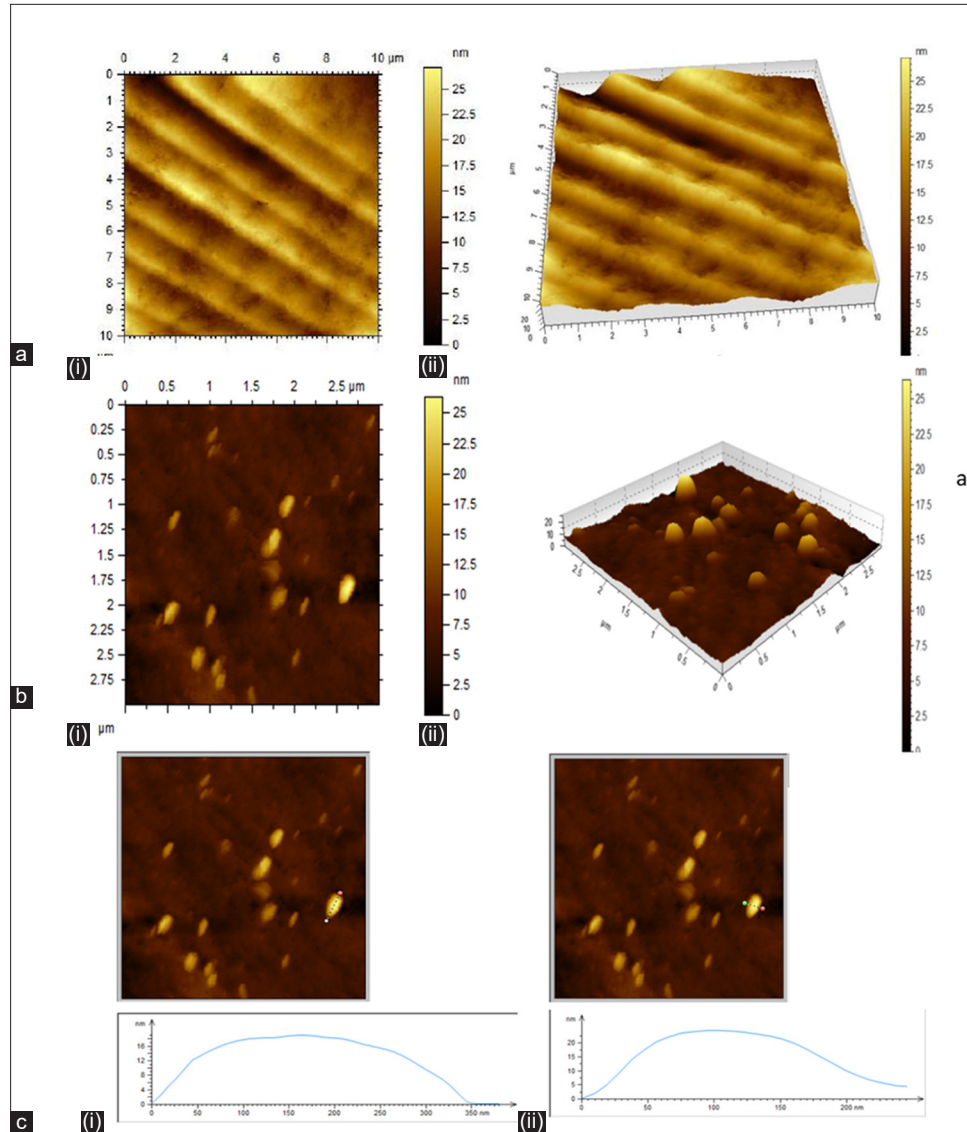


Figure 5: Atomic force microscopy image analysis of vas fluid; a (i) 2D and (ii) 3D image of processed vas fluid from control rats. b (i) 2D and (ii) 3D images of processed vas fluid from implant-injected rats. c (i) and (ii) dimension profile analysis of two selected liposomal structures.

Full product ion scan of FIN standard with the precursor ion m/z 373 corresponding to $[M+H]^+$ resulted in two main product ions at m/z 317 and 305 [Figure 6a (i) and (ii)]. The control group, which was not subjected to any treatment or implant injection did not show up the characteristic mass spectra peak for FIN [Figure 6b (i)]. The analysis of the prostate tissue extract from the implant injected group detected a peak for an m/z ratio of 373.679 corresponding to $[M+H]^+$ of FIN [Figure 6c (i)], showing the presence of FIN molecules in the prostate tissue. The corresponding $[M+H]^+$ precursor ion showed two ion fragments at m/z 317 and 305 when subjected to MS/MS analysis [Figure 6c (ii)].

The characteristic $[M+H]^+$ precursor ion of FIN and its corresponding elemental composition were analyzed by HRMS [Figure 7a]. The standard FIN showed observed and calculated $[M+H]^+$ values of 373.2868 and 373.2855, respectively, with an error of +3.5 ppm corresponding to the mono-protonated FIN ($C_{23}H_{37}O_2N_2$).

On the other hand, the implant injected sample showed the ion peak with the m/z value of 373.2828 [Figure 7b], which differs from the exact mono-protonated mass value of FIN by -7.2 ppm. The elemental composition of the observed m/z peak of the sample isolated from implant-injected rat was identical with the standard FIN composition well within the tolerance level [Figure 7c].

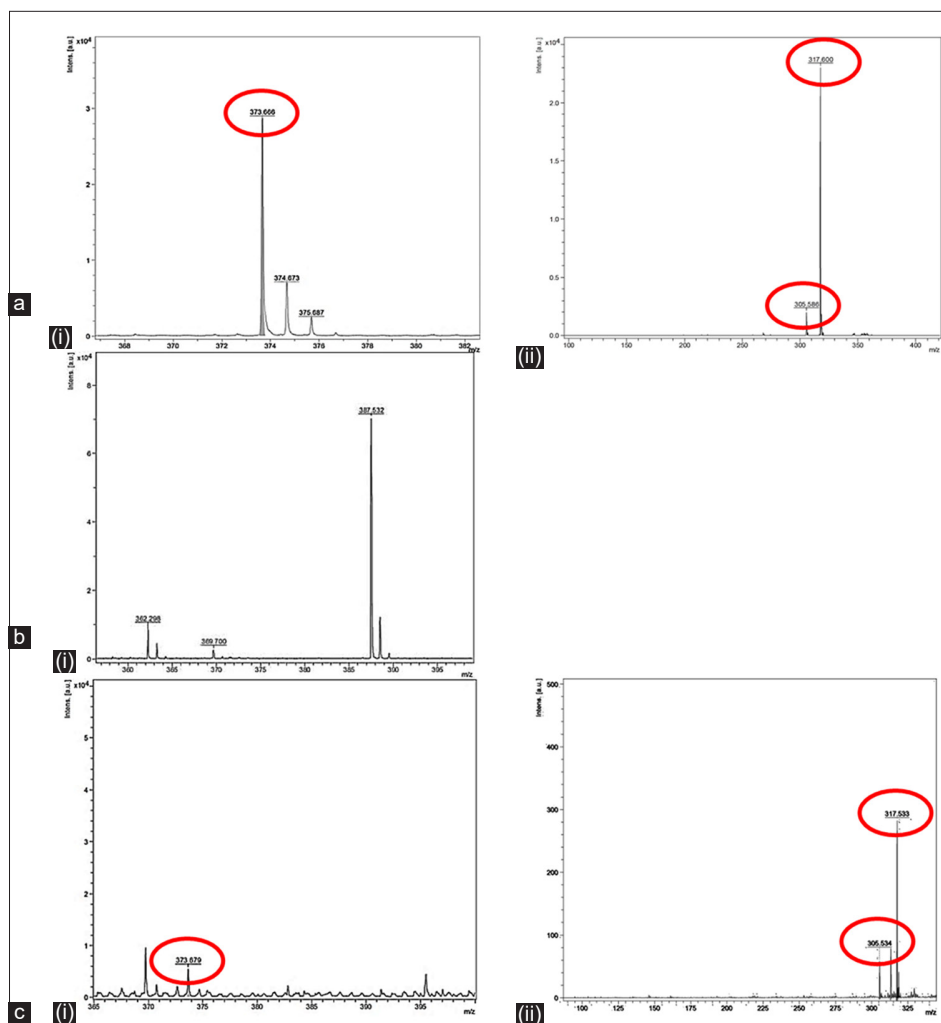


Figure 6: MALDI-ToF/ToF of standard FIN, a (i), MS; (ii), MS/MS of $[M+H]^+$; (b) control prostate tissue extract; prostate tissue extract of implant injected rat, c (i), MS; (ii), MS/MS of $[M+H]^+$, where $M = 372$ and $[M+H]^+ = 373$. Precursor ion of FIN m/z (373) and corresponding product ions of the precursor ion ($373 \rightarrow 317$ and 305). MALDI-ToF/ToF: Matrix-assisted laser desorption ionization-time of flight, FIN: Finasteride, MS: Mass spectrometry. x: Intensity, y: mass/charge ratio.

DISCUSSION

Biophysical characterization of the implant by FTIR and PXRD showed the complex formation between FIN and SMA: DMSO. FIN interacted with SMA by carbonyl (C=O) amide of FIN, suggesting the interaction of FIN with the SMA component by intermolecular hydrogen bonding.^[27] The FIN molecule also interacted with the acid group of SMA formed by converting anhydride to the acid group, suggesting the involvement of hydrogen bonding. FIN was also shown to interact with the sulfoxide group of DMSO, which is characterized by a shift in frequency from 1042 cm^{-1} to 1025 cm^{-1} . Such a shift in frequency to a longer wavelength is attributed to the oxygen atom in DMSO.^[23,25] Based on the shifts in the transmittance peak of the implant

components, it can be inferred that a complex is formed due to the intermolecular interaction taking place among the system's three components, ultimately resulting in the encapsulation of FIN in the polymer matrix.

The presence of the characteristic peak at $19.60\ 2\theta$ of FIN [Figure 3b] with a marked decrease in intensity in the implant confirmed the semi-crystalline state of the drug in the implant. The semi-crystalline state offers long-term stability over amorphous for long-term drug delivery and the physiological environment where this DDS is implanted. As with poorly water-soluble drugs, the amorphous nature of the drug is a prerequisite for improving the bioavailability, particularly when the drug is administered orally.^[28,29] Herein, the drug encapsulated in the polymer matrix is injected into the

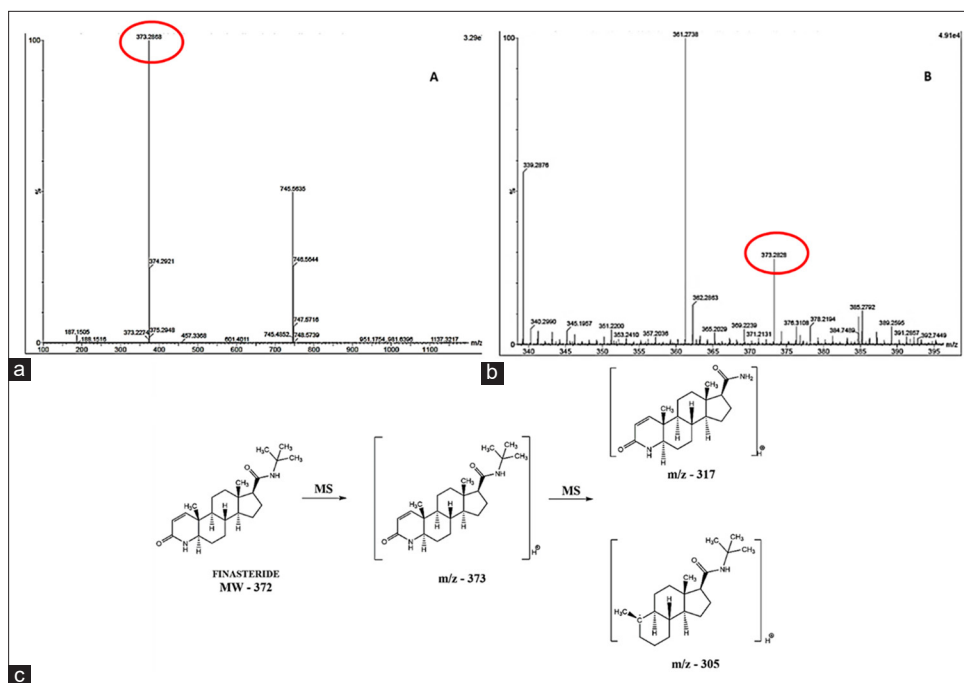


Figure 7: HRMS of (a) standard FIN; (b) prostate tissue extract of implant injected rat. (c) Structural representation of the fragmentation pattern of FIN subjected to MS/MS analysis. HRMS: High-resolution mass spectrometry, FIN: Finasteride, MS: Mass spectrometry.

lumen of the vas deferens, where the vas fluid is constantly replenished and reabsorbed. Consequently, the amorphous form of the drug will tend to dissolve easily and quickly, which will not be useful from the perspective of long-term delivery of the drug. Thus, the semi-crystal state of the drug is essential for the existence of the drug in the vas to fulfill the objective of long-term drug delivery with a one-time injection of the implant in the vas deferens.

SMA has been shown to form stable self-assembled nano to micron-sized structures of different geometries.^[30-32] Here, our study utilizes the mechanistic concept of RISUG[®], which disrupts the sperm cell plasma membrane.^[17] We formulated an implant that remains lodged in of vas deferens' lumen and forms nanoparticles that encapsulate the drug-polymer complex. The nano- and sub-micron-sized self-assembled particles are generated and are encapsulated by the phospholipids derived from the sperm cell plasma membrane, leading to the formation of polymer-drug complex encapsulated liposomes. The presence of submicron-sized particles observed by AFM and fluorescent microscopy confirmed the generation of such particles inside the vas deferens. It indicates that the particles that are generated inside the vas have a varying size in the submicron range from 100 nm to 700 nm [Figure 5c]. The presence of a globular structure confirms the concept of *in vivo* formation of nanoparticles. The presence of lipid components in the particles that are forming could be confirmed by the Nile

red staining, which binds to lipids, esterified cholesterol, and triglyceride, and its intensity increases with the increase in the hydrophobic environment.^[33,34]

MALDI-ToF study confirmed the presence of a peak at m/z 373.679 corresponding to the $[M+H]^+$ of FIN. The absence of the characteristic peak in the control rats confirmed the absence of FIN or other molecules with similar mass in the ventral prostate tissue. To further confirm the drug molecule, $[M+H]^+$ ion was subjected to MS/MS analysis, which showed production at 317 and 305, similar to that obtained for the standard FIN. These two product ions are representative of precursor ions of FIN molecule when subjected to MS/MS analysis confirming the molecule and hence have been used for both qualitative and quantitative studies in pharmacokinetic studies pertaining to FIN^[29] [Figure 7c]. For further confirmation of the presence of FIN in the implant-injected rats, the elemental composition of the corresponding $[M+H]^+$ precursor ion of FIN was studied by HRMS. The implant injected group showed the presence of $[M+H]^+$ precursor ion with an actual mass error of -7.2 ppm and elemental composition of $C_{25}H_{37}O_2N_2$ corresponding to the elemental composition of standard FIN precursor ion $[M+H]^+$ with an actual mass error of 3.5 ppm.

Another interesting observation in this study was that the drug was detected in the ventral prostate of the rats after 28 days of implant injection. In this study, two different doses of FIN were used in a stoichiometric ratio

Table 1: Assignment of transmittance peak of components of FIN, SMA, DMSO, FIN: DMSO, SMA: DMSO, and SMA: FIN: DMSO (Implant).

Sample	IR Transmittance band/cm ⁻¹	Description
FIN	3429 3241 1687 1600	vas (NH ₂) vs (NH ₂) v (C=O) amide v C=C (aromatic ring stretching)
SMA	1771 1218 1491.70 1450.47 700	vs C=O anhydride v (C-O-C) of maleic anhydride δ C=C vibration of phenyl ring (characteristic of styrene)
DMSO	1437 1407 1312 1042	δ _{as} CH ₃ δ _{as} CH ₃ δ _s CH ₃ v S=O
SMA+DMSO	2913 1663 1312 1036 954.51	v C-H stretching v (C=O) δ _{as} CH ₃ v S=O CH bending
FIN+DMSO	3422 1025	vas (NH ₂) (red shift) v S=O (red shift)
SMA+FIN+DMSO (DDS/Implant)	1667 1223 1600 1023	v (C=O) amide (red shift) v C=C (aromatic ring stretching) v S=O (red shift)

FIN: Finasteride, SMA: Styrene maleic anhydride, DMSO: Dimethyl sulfoxide, DDS: Drug delivery system, v: Symmetric stretching, vas: Asymmetric stretching, δ_s: Symmetric bending, δ_{as}: Antisymmetric bending, IR: Infrared

of 1:0.5:10 and 1:1:10 for SMA: FIN: DMSO implant. The drug was detected after 28 days of injection 1:1:10 ratio group had 50 µL of implant injected, which corresponds to a total of 5.0 mg of FIN (2.5 mg/25 µL in each vas deferens), [Figures 6 and 7, Figure S2]. Considering the pharmacokinetic parameter for oral administration of FIN with a half lifetime of 2.2 h in rats showed a decreased concentration of FIN due to its low half-life ($T_{1/2}$).^[35] Based on the pharmacokinetic information, the detection of FIN in the ventral prostate suggests that FIN reached the target tissue over a long period and substantiated the concept of a drug depot formation in the vas deferens lumen, which possibly facilitated its sustained release as confirmed by

MALDI-ToF study. This correlates with a decrease in the wet weight of the ventral prostate of implant-injected rats compared to the control rats over 28 days [Figure S1 and Table S1]. Interestingly, when 5 mg of FIN was administered orally in rats, after 10 days, the FIN detection level was almost negligible, whereas in implant-injected rats, the FIN was detected in the prostate with good signal intensity in both up to 28 days. The percentage decrease in prostate wet weight was also less compared to the 14 days and 28 days groups. This showed that this mode of drug delivery offers an advantage over the oral route of drug delivery and should be explored further. The study has few limitations due to differences in human and rat vas deferens anatomical and vasculature differences. We have not explored in detail the nanoparticle distribution in the prostate and the micro-route that facilitates such transport from the vas deferens to the prostate. All these aspects need future exploration to further develop the locoregional delivery of drugs to the prostate.

CONCLUSION

Our study presents RISUG-PH™ as a novel vas injectable implant that facilitates delivery of FIN to the ventral prostate through the vas deferens in male rats. The present study demonstrates an innovative approach for sustained drug release and introduces the concept of invivgensome, where self-assembled nanoparticles are generated within the body through an implant-directed mechanism. The detection of FIN in the prostate after 28 days post-implantation underscores the long-term delivery of the drug, underscoring the significance of this method in developing therapy for BPH. Our findings highlight RISUG-PH™ as a promising alternative for prolonged drug delivery, requiring further investigation into the biochemical and biophysical properties of invivgensomes and the underlying mechanisms governing drug transport. Future research requires detailed biochemical and biophysical characterization of the nanoparticles/microparticles and elucidating the mechanism by which the drug is delivered to the prostate from vas deferens.

Acknowledgment: We acknowledge the Central Research Facility, Indian Institute of Technology (IIT), Kharagpur, and Department of Chemistry (IIT- Kharagpur) for their experimental contribution.

Ethical approval: The research/study approved by the Institutional Animal Ethics Committee at School of Medical Science and Technology, Indian Institute of Technology Kharagpur, 2015.

Declaration of patient consent: Patient's consent was not required as there are no patients in this study.

Financial support and sponsorship: This work was supported by the Ministry of Health and Family Welfare, Government of India (M11011/2/2008-FP).

Conflicts of interest: Sujoy K. Guha is on the Editorial Board of the Journal.

Use of artificial intelligence (AI)-assisted technology for manuscript preparation: The authors confirm that there was no use of artificial intelligence (AI)-assisted technology for assisting in the writing or editing of the manuscript, and no images were manipulated using AI.

REFERENCES

1. Ørsted DD, Bojesen SE. The link between benign prostatic hyperplasia and prostate cancer. *Nat Rev Urol* 2013;10:49-54.
2. Bray F, Laversanne M, Sung H, Ferlay J, Siegel RL, Soerjomataram I, *et al.* Global cancer statistics 2022: GLOBOCAN estimates of incidence and mortality worldwide for 36 cancers in 185 countries. *CA Cancer J Clin* 2024;74: 229-63.
3. Ezike TC, Okpala US, Onoja UL, Nwike CP, Ezeako EC, Okpara OJ, *et al.* Advances in drug delivery systems, challenges and future directions. *Heliyon* 2023;9:e17488.
4. Traish AM, Hassani J, Guay AT, Zitzmann M, Hansen ML. Adverse side effects of 5 α -reductase inhibitors therapy: Persistent diminished libido and erectile dysfunction and depression in a subset of patients. *J Sex Med* 2011;8:872-84.
5. Traish AM, Mulgaonkar A, Giordano N. The dark side of 5 α -reductase inhibitors' therapy: Sexual dysfunction, high Gleason grade prostate cancer and depression. *Korean J Urol* 2014;55:367-79.
6. Tibbitt MW, Dahlman JE, Langer R. Emerging frontiers in drug delivery. *J Am Chem Soc* 2016;138:704-17.
7. Shaha S, Rodrigues D, Mitragotri S. Locoregional drug delivery for cancer therapy: Preclinical progress and clinical translation. *J Control Release* 2024;367:737-67.
8. Gao J, Karp JM, Langer R, Joshi N. The future of drug delivery. *Chem Mater* 2023;35:359-63.
9. Koslov D, Andersson KE. Physiological and pharmacological aspects of the vas deferens-An update. *Front Pharmacol* 2013;4:101.
10. Kimura Y, Adachi K, Kasaki N, Ise K. On the transportation of spermatozoa in the vas deferens. *Andrologia* 1975;7:55-61.
11. Skinner JD, Rowson LE. Effects of testosterone injected unilaterally down the vas deferens on the accessory glands of the ram. *J Endocrinol* 1968;42:355-6.
12. Ohtani O, Gannon BJ. The microvasculature of the rat vas deferens: A scanning electron and light microscopic study. *J Anat* 1982;135:521-9.
13. Pierrepont CG, Davies P. The effect of vasectomy on the activity of prostatic RNA polymerase in rats. *J Reprod Fertil* 1973;35:149-52.
14. Pierrepont CG, Davies P, Wilson DW. The role of the epididymis and ductus deferens in the direct and unilateral control of the prostate and seminal vesicles of the rat. *J Reprod Fertil* 1974;41:413-23.
15. Pierrepont CG, Davies P, Millington D, John B. Evidence that the deferential vein acts as a local transport system for androgen in the rat and the dog. *J Reprod Fertil* 1975;43:293-303.
16. Guha SK. Contraceptive for use by a male; 1994. Available from: <https://patentimages.storage.googleapis.com/14/7d/3f/0444ba10d18781/US5488075.pdf> [Last accessed on 2024 Feb 05].
17. Chaudhury K, Bhattacharyya AK, Guha SK. Studies on the membrane integrity of human sperm treated with a new injectable male contraceptive. *Hum Reprod* 2004;19:1826-30.
18. Guha SK. Drug delivery system for finasteride to prostate. US Patent WO2013124865A1; 2013.
19. Maeda K, Ohkura S, Tsukamura H. Chapter 9-Physiology of reproduction. In: Krinke GJ, editor. *Handbook of animal models of infection*. London: Academic Press; 2000. p. 145-76.
20. Lohiya NK, Suthar R, Khandelwal A, Goyal S, Ansari AS, Manivannan B. Sperm characteristics and teratology in rats following vas deferens occlusion with RISUG and its reversal. *Int J Androl* 2010;33:e198-206.
21. Constanzer ML, Chavez CM, Matuszewski BK. Picogram determination of finasteride in human plasma and semen by high-performance liquid chromatography with atmospheric-pressure chemical-ionization tandem mass spectrometry. *J Chromatogr B Biomed Sci Appl* 1994;658:281-7.
22. Wawrzycka I, Stępnik K, Matyjaszczyk S, Kozioł AE, Lis T, Abboud KA. Structural characterization of polymorphs and molecular complexes of finasteride. *J Mol Struct* 1999;474: 157-66.
23. Fawcett WR, Kloss AA. Solvent-induced frequency shifts in the infrared spectrum of dimethyl sulfoxide in organic solvents. *J Phys Chem* 1996;100:2019-24.
24. Yamauchi H, Maeda Y. LCST and UCST behavior of poly(*N*-isopropylacrylamide) in DMSO/water mixed solvents studied by IR and micro-Raman spectroscopy. *J Phys Chem B* 2007;111:12964-8.
25. Schoukens G, Martins J, Samyn P. Insights in the molecular structure of low- and high-molecular weight poly(styrene-maleic anhydride) from vibrational and resonance spectroscopy. *Polymer (Guildf)* 2013;54:349-62.
26. Jha RK, Jha PK, Guha SK. Smart RISUG: A potential new contraceptive and its magnetic field-mediated sperm interaction. *Int J Nanomedicine* 2009;4:55-64.
27. Shundalau M, Chybirai PS, Komyak AI, Zazhugin AP, Umreiko DS. Structure and vibrational IR spectra of a UCl₄-2DMSO complex. *J Appl Spectrosc* 2012;79:165-72.
28. Babu NJ, Nangia A. Solubility advantage of amorphous drugs and pharmaceutical cocrystals. *Cryst Growth Des* 2011;11:2662-79.
29. Lundahl A, Lennernäs H, Knutson L, Bondesson U, Hedeland M. Identification of finasteride metabolites in human bile and urine by high-performance liquid chromatography/tandem mass spectrometry. *Drug Metab Dispos* 2009;37:2008-17.
30. Tao M, Hu Z, Zhang Z. Morphology of the poly (styrene-alt-maleic anhydride) micelles obtained by radiation-induced emulsion polymerization using anionic/nonionic mixed surfactants templates. *Mater Lett* 2008;62:597-9.
31. Lazzara TD, Whitehead MA, van de Ven TG. Linear nano-templates of styrene and maleic anhydride alternating copolymers. *Eur Polym J* 2009;45:1883-90.
32. Malardier-Jugroot C, van de Ven TG, Whitehead MA. Linear conformation of poly (styrene-alt-maleic anhydride) capable of self-assembly: A result of chain stiffening by internal hydrogen bonds. *J Phys Chem B* 2005;109:7022-32.
33. Greenspan P, Mayer EP, Fowler SD. Nile red: A selective

fluorescent stain for intracellular lipid droplets. *J Cell Biol* 1985;100:965-73.

34. Diaz G, Melis M, Batetta B, Angius F, Falchi AM. Hydrophobic characterization of intracellular lipids *in situ* by Nile Red red/yellow emission ratio. *Micron* 2008;39:819-24.
35. Stuart JD, Lee FW, Noel DS, Kadwell SH, Overton LK, Hoffman CR, *et al.* Pharmacokinetic parameters and mechanisms of inhibition of rat type 1 and 2 steroid

5 α -reductases: Determinants for different *in vivo* activities of G1198745 and finasteride in the rat. *Biochem Pharmacol* 2001;62:933-42.

How to cite this article: Gupta S, Bisevac J, Guha SK. Qualitative study for finasteride detection in the prostate delivered by reversible inhibition of sperm under guidance – Prostate hair (RISUG-PH™) vas injectable implant. *J Reprod Healthc Med* 2025;6:11. doi: 10.25259/JRHM_2_2024